PSFC/JA-97-16

Edge Emittance Growth and Particle Diffusion Induced by Discrete-Particle Effects in Intense Beam Simulations

Renato Pakter and Chiping Chen

July, 1997

Plasma Science and Fusion Center
Massachusetts Institute of Technology
Cambridge, MA 02139, USA

This research was supported by Department of Energy Grant No. DE-FG02-95ER-40919, and Air Force Office of Scientific Research Grant Nos. F49620-94-1-0374 and F49620-97-1-0325. The Research by R. Pakter was also supported by CAPES, Brazil.

Submitted for publication in *Physical Review Letters*.

Edge Emittance Growth and Particle Diffusion Induced by Discrete-Particle Effects in Intense Beam Simulations

Renato Pakter and Chiping Chen

Plasma Science and Fusion Center

Massachusetts Institute of Technology

Cambridge, Massachusetts 02139

(July 7, 1997)

Abstract

We analyze particle diffusion and edge emittance growth induced by discrete-particle effects in two-dimensional self-consistent simulation studies of beam dynamics. In particular, an analytical model is presented which describes the slow-time-scale evolution of the edge emittance of a perfectly matched beam in a periodic solenoidal magnetic field. A scaling law for edge emittance growth is derived analytically and confirmed by self-consistent simulations. Applications of the scaling law are discussed.

29.27.-a,41.75.-i,07.05.Tp

Typeset using REVTEX

High-current electron and ion accelerators are the subject of vigorous research [1,2] because their applications in high-energy and nuclear physics research, coherent radiation generation, heavy ion fusion, and tritium production. Although self-consistent computer simulation codes are widely used in the basic studies and design of advanced high-current accelerators [3-10], it remains challenging to make accurate predictions of beam losses [9] and emittance growth because of numerical noise in the simulations. Numerical noise is caused primarily by discrete-particle effects (i.e., effects associated with intrabeam scattering among discrete particles) resulted from the fact that the number of particles employed in the simulation is limited. In the regime where collective effects play an important role in the beam dynamics, numerical noise imposes a particularly serious problem in simulating dynamical processes (e.g., beam losses) involving the tail of the distribution function. Several analyses [11-13] have been reported of the intrabeam scattering problem using the Fokker-Planck equation. The analyses provide a general framework for studies of the intrabeam scattering problem, either physical or numerical, but require detailed knowledge of diffusion coefficients which are available only for beams with a Maxwellian distribution in velocity space.

In this Letter, we present a theory describing the slow-time-scale evolution of the transverse edge emittance in a self-consistent two-dimensional model of a continuous intense charged-particle beam propagating through a periodic solenoidal focusing field. In particular, a complete set of self-consistent, slow-time-scale equations of motion is derived to describe the nonlinear dynamics of macroparticles in an intense beam. Assuming that the beam is perfectly matched into the periodic focusing field in the limit of a smooth equilibrium distribution corresponding to the Kapchinskij-Vladimirskij (KV) equilibrium [14,15], and performing statistical averages, we obtain an analytical scaling law governing transverse edge emittance growth induced by discrete-particle effects. The scaling law is verified by comparing with self-consistent simulations. Possible applications of the scaling law are discussed. With some straightforward generalization, the technique presented in this paper can be applied in simulation studies of a wide range of charged-particle beam and nonneutral plasma systems.

We consider a thin, continuous charged-particle beam which propagates with average axial velocity $\beta_b c\vec{e}_z$ through an axisymmetric linear focusing channel provided by a periodic solenoidal magnetic field

$$\vec{B}_0(x,y,s) = B_z(s)\,\vec{e}_z - \frac{1}{2}B_z'(s)(x\vec{e}_x + y\vec{e}_y). \tag{1}$$

In Eq. (1) $s = z = \beta_b ct$ is the axial coordinate, $B_z(s+S) = B_z(s)$ is the axial component of the applied magnetic field, S is the fundamental periodicity length of the focusing field, c is the speed of light *in vacuo*, and prime denotes derivative with respect to s.

In the present two-dimensional macroparticle model, the beam density is given by

$$n(x,y,s) = \frac{N}{N_p}\sum_{i=1}^{N_p}\delta[x - x_i(s)]\,\delta[y - y_i(s)], \tag{2}$$

where N is the number of microparticles per unit axial length of the beam, N_p is the number of macroparticles used in the simulation, and (x_i, y_i) is the transverse displacement of the ith macroparticle from the beam axis at $(x,y) = (0,0)$. Under the paraxial approximation, we can express the transverse equations of motion for the ith macroparticle in the Larmor frame as [8]

$$\frac{d^2\tilde{x}_i}{ds^2} + \kappa_z(s)\,\tilde{x}_i = -\frac{q}{\gamma_b^3\beta_b^2 mc^2}\frac{\partial}{\partial\tilde{x}_i}\Phi^s(\tilde{x}_i,\tilde{y}_i,s), \tag{3}$$

$$\frac{d^2\tilde{y}_i}{ds^2} + \kappa_z(s)\,\tilde{y}_i = -\frac{q}{\gamma_b^3\beta_b^2 mc^2}\frac{\partial}{\partial\tilde{y}_i}\Phi^s(\tilde{x}_i,\tilde{y}_i,s). \tag{4}$$

In Eqs. (3) and (4), $i = 1,2,...,N_p$, $(\tilde{x},\tilde{y})$ is the Larmor-frame coordinate, $\gamma_b = (1-\beta_b^2)^{-1/2}$ is the relativistic mass factor, m and q are the particle rest mass and charge, respectively, $\kappa_z(s) = [qB_z(s)/2\gamma_b\beta_b mc^2]^2$ is a measure of the strength of the focusing field, and

$$\Phi^s(\tilde{x}_i,\tilde{y}_i,s) = -\frac{qN}{N_p}\sum_{j=1(j\neq i)}^{N_p}\ln[(\tilde{x}_i-\tilde{x}_j)^2 + (\tilde{y}_i-\tilde{y}_j)^2] \tag{5}$$

is the self-field scalar potential associated with the beam space-charge.

In order to develop an analytical model to describe diffusive behavior induced by discrete-particle effects in beam dynamics, we first consider the limit of a *smooth* equilibrium distribution of particles corresponding to the KV equilibrium [14,15]. In the KV equilibrium, the beam density is given by

$$n_{KV}(\tilde{x},\tilde{y},s) = \begin{cases} N/\pi r_b^2(s), & 0 \leq r \leq r_b(s), \\ 0, & r > r_b(s), \end{cases} \tag{6}$$

where $r \equiv (x^2+y^2)^{1/2} = (\tilde{x}^2+\tilde{y}^2)^{1/2}$ is the radial coordinate, and $r_b = r_b(s)$ is the beam radius. The scalar potential for the self-electric field is given by

$$\Phi^s_{KV}(\tilde{x},\tilde{y},s) = -\frac{qNr^2}{r_b^2(s)} \tag{7}$$

in the beam interior ($r < r_b$). Substituting $\Phi^s(\tilde{x}_i,\tilde{y}_i,s) = \Phi^s_{KV}(\tilde{x}_i,\tilde{y}_i,s)$ into Eqs. (3) and (4), it can be shown that the equilibrium particle orbits $\tilde{x}_i(s)$ and $\tilde{y}_i(s)$ can be expressed as [15]

$$\tilde{x}_i(s) = A_{xi}\, r_b(s) \cos[\psi(s) + \phi_{xi}], \tag{8}$$

$$\tilde{y}_i(s) = A_{yi}\, r_b(s) \sin[\psi(s) + \phi_{yi}], \tag{9}$$

where A_{xi} $(0 \leq A_{xi} \leq 1)$, $A_{yi} = (1 - A_{xi}^2)^{1/2}$, ϕ_{xi} and ϕ_{yi} are all constants determined by the initial conditions, $\psi(s) = 4\epsilon \int_0^s ds/r_b^2(s)$ is the accumulated phase of the betatron oscillations, and $r_b(s) = r_b(s+S)$ solves the beam envelope equation

$$\frac{d^2 r_b}{ds^2} + \kappa_z(s)\, r_b - \frac{K}{r_b} - \frac{(4\epsilon)^2}{r_b^3} = 0, \tag{10}$$

with ϵ being the unnormalized rms emittance of the beam (without factor of 4), and $K \equiv 2q^2N/\gamma_b^3\beta_b^2 mc^2$, the normalized perveance of the beam. The KV equilibrium distribution function can be expressed as $f_{KV}(\tilde{x},\tilde{y},\tilde{x}',\tilde{y}',s) = (N/16\epsilon^2\pi^2)\,\delta(A_x^2 + A_y^2 - 1)$, where $\delta(x)$ is the Dirac δ-function. Because the four-dimensional phase-space volume element is given by $d\tilde{x}d\tilde{y}d\tilde{x}'d\tilde{y}' = 16\epsilon^2 A_x\, A_y\, dA_x dA_y d\phi_x d\phi_y$, integrating f_{KV} over A_y, ϕ_x and ϕ_y yields the distribution function for A_x over the KV beam

$$F_{KV}(A_x) = \begin{cases} 2NA_x, & 0 \le A_x \le 1, \\ 0, & A_x > 1, \end{cases} \tag{11}$$

where $\int_0^\infty F_{KV}(A_x)dA_x = N$. Note from Eq. (11) that the largest concentration of particles occurs at $A_x = 1$. Note also from Eq. (8) that particles with $A_{xi} = 1$ reach the edge of the beam with $\tilde{x}_i = r_b$, as they execute betatron oscillations. Therefore, they are most likely to leave the beam core under the perturbations induced by discrete-particle effects.

In numerical simulations, the beam density deviates from the smooth beam density $n_{KV}(\tilde{x}, \tilde{y}, s)$ of the KV equilibrium. For a coarse-grained uniform density distribution, the deviation is small when there is a large number of macroparticles. Such small deviation will induce slow-time-scale evolution of $A_{xi}(s)$, $A_{yi}(s)$, $\phi_{xi}(s)$ and $\phi_{yi}(s)$ in the particle orbits given in Eqs. (8) and (9). In the remainder of this paper, we focus our attention to the dynamics of edge particles initially with $A_{xi}(0) = 1$ and $A_{yi}(0) = [1 - A_{xi}^2(0)]^{1/2} = 0$, because they are most likely to diffuse away from the beam core as discussed previously. We disregard dynamical couplings between (A_{xi}, ϕ_{xi}) and (A_{yi}, ϕ_{yi}) because $A_{yi}(s) \approx 0$, and introduce the dimensionless variables and parameters defined by $s/S \to s$, $\tilde{x}/(4\epsilon S)^{1/2} \to \tilde{x}$, $\tilde{y}/(4\epsilon S)^{1/2} \to \tilde{y}$, $r_b/(4\epsilon S)^{1/2} \to r_b$, $S^2\kappa_z \to \kappa_z$ and $SK/4\epsilon \to K$. Unless specified, the dimensionless variables and parameters will be used hereafter. Substituting Eq. (8) into Eq. (3), and taking into account the *slow* dependence of A_{xi} and ϕ_{xi}, we find that

$$\left[A'_{xi} r'_b - \frac{A_{xi}\phi'_{xi}}{r_b}\right]\cos(\psi + \phi_{xi}) - \left[\frac{A'_{xi}}{r_b} + A_{xi}\phi'_{xi} r'_b\right]\sin(\psi + \phi_{xi}) = -\frac{K}{4qN}\frac{\partial}{\partial x_i}\left[\Phi^s - \Phi^s_{KV}\right], \tag{12}$$

where use has been made of Eq. (10), and Φ^s and Φ^s_{KV} are defined in Eqs. (5) and (7), respectively. It is evident in Eq. (12) that $A'_{xi} = 0 = \phi'_{xi}$ for $\Phi^s = \Phi^s_{KV}$.

To derive a closed set of equations for the slowly varying variables A_{xi} and ϕ_{xi}, we average Eq. (12) over fast oscillations pertaining to the focusing field and the betatron oscillations. Making use of Eqs. (5) and (7)-(9), we can express Eq. (12) as

$$\frac{dA_{xi}}{ds} = -\frac{K}{N_p}\sum_{j=1(j\neq i)}^{N_p}\frac{B_j b_j + C_j c_j}{b_j^2 + c_j^2}, \tag{13}$$

$$\frac{d\phi_{xi}}{ds} = \frac{K}{2} - \frac{K}{A_{xi}N_p} \sum_{j=1(j\neq i)}^{N_p} \frac{C_j b_j - B_j c_j}{b_j^2 + c_j^2}, \tag{14}$$

where

$$B_j = -(A_{xj}/2)\sin\Delta_{xj}, \quad C_j = (A_{xi} - A_{xj}\cos\Delta_{xj})/2,$$

$$b_j = [(A_{xi} - A_{xj}\cos\Delta_{xj})^2 - A_{xj}^2 \sin^2\Delta_{xj} - A_{yj}^2\cos(2\Delta_{yj})]/2, \tag{15}$$

$$c_j = (A_{xi} - A_{xj}\cos\Delta_{xj})A_{xj}\sin\Delta_{xj} + A_{yj}^2\sin(2\Delta_{yj})/2,$$

with $\Delta_{xj} \equiv \phi_{xj} - \phi_{xi}$ and $\Delta_{yj} \equiv \phi_{yj} - \phi_{xi}$. Since the derivation of Eqs. (13) and (14) does not require the explicit form of the focusing magnetic field $B_z(s)$, Eqs. (13) and (14) are valid for an arbitrary periodic magnetic field.

In principle, detailed dynamics of edge particles initially with $A_{xi} = 1$ and $A_{yi} = 0$ can be analyzed using Eqs. (13) and (14). In this paper, however, we examine particularly particle diffusion induced by discrete-particle effects. To describe the diffusion process quantitatively, we introduce the quantities $\mu(s) = \langle A_{xi} \rangle$ and $\sigma_A^2(s) = \langle (A_{xi} - \mu)^2 \rangle$, where $\langle\ \rangle$ stands for the average over particles that are initially located at $A_{xi} = 1$. We compute the expectation values of $d\mu/ds = \langle A'_{xi} \rangle$ and $d^2\sigma_A^2/ds^2 = 2\langle (A'_{xi} - \mu')^2 \rangle$ by ensemble averaging over all possible beam distributions which approach the KV distribution when $N_p \to \infty$. The results are $\mu(s) = \mu(0) = 1$, and

$$\sigma_A^2(s) = D\, s^2, \tag{16}$$

where the coefficient D is defined by

$$D(K, N_p) = \frac{\overline{\xi}\, K^2}{N_p}. \tag{17}$$

Here, $\overline{\xi} = (1/N)\int \xi_j f_{KV}(\tilde{x}_j, \tilde{y}_j, \tilde{x}'_j, \tilde{y}'_j, s) d\tilde{x}_j d\tilde{y}_j d\tilde{x}'_j d\tilde{y}'_j$ and $\xi_j = [(B_j b_j + C_j c_j)/(b_j^2 + c_j^2)]^2$. It should be stressed that unlike usual diffusive processes, the variance σ_A^2 here is proportional to s^2. Due to the highly oscillatory nature of ξ_j, our best estimate of the value of $\overline{\xi}$ is $\overline{\xi} = 0.7 \pm 0.3$.

The results in Eqs. (16) and (17) can be interpreted in terms of dimensional variables and parameters as follows. Let us define the edge emittance $4\epsilon_{max}$ of the beam as the ensemble average value of the areas encircled by the edge particles in the phase space $(\tilde{x}, \tilde{x}')$ divided by π. Since $A_{xi}(0) = 1$ for all of the edge particles and the area encircled by the ith edge particle is $4\pi\epsilon A_{xi}^2(s)$, it follows from Eqs. (16) and (17) that the edge emittance of the beam evolves according to the following (dimensional) equation

$$4\epsilon_{max}(s) = 4\epsilon_{max}(0)\left[1 + \frac{\overline{\xi} K^2 s^2}{16\epsilon_{max}^2(0) N_p}\right], \tag{18}$$

where $\overline{\xi} = 0.7 \pm 0.3$, $\epsilon_{max}(0) = \epsilon$, and $K = 2q^2N/\gamma_b^3\beta_b^2 mc^2$. Equation (18) is the key result of this paper.

To verify the scaling law in Eqs. (16) and (17), we carry out self-consistent simulations by integrating Eqs. (3) and (4) numerically for various particle distributions. We adopt the following procedure to calculate particle diffusion about $A_{xi} = 1$. In such a self-consistent simulation, a first set of N_p macroparticles is loaded corresponding to a KV distribution, a second set of N_t test particles is loaded at $A_{xi}(0) = 1$ with a uniform distribution of $\phi_{xi}(0)$ in the range from 0 to 2π. As the beam propagates through the focusing channel, the particles in the first set interact with each other self-consistently, whereas the test particles experience the electric and magnetic forces imposed by the particles in the first set. Integrating Eq. (10) concurrently to obtain the radius for the match beam in the simulation, and using the relation $A_{xi} = [(\tilde{x}_i/r_b)^2 + (\tilde{x}_i r_b' - \tilde{x}_i' r_b)^2]^{1/2}$, the expectation values of $\mu(s)$ and $\sigma_A^2(s)$ over the test-particle distribution are computed. Results are summarized in Figs. 1-3.

Figure 1 shows a plot of σ_A^2/s^2 versus the normalized propagation distance s obtained from a self-consistent simulation of intense beam propagation through a sinusoidal periodic focusing channel. The choice of system parameters in Fig. 1 corresponds to $N_p = 1024$, $N_t = 512$, $K = 0.5$, and $\kappa_z(s) = [a_0 + a_1\cos(2\pi s)]^2$, where $a_0 = a_1 = 0.648$. Due to small residual correlation in the initial distributions of test particles and background macroparticles, the value of σ_A^2/s^2 is large for $s \ll 1$. As the beam propagates, the residual correlation decays rapidly, and the value of σ_A^2/s^2 approaches a plateau for $s > 1$ indicated by the dashed line, where the coefficient D is evaluated to be $D = 1.0 \times 10^{-4}$ ($\bar{\xi} = 0.4$). As the beam propagates further through the focusing channel, the plateau levels off because the test particles become widely spread about $A_{xi} = 1$.

The scaling law is verified by self-consistent simulations. Figure 2 shows a logarithmic plot of D versus K obtained from self-consistent simulations for beam propagation through the same periodic focusing channel as in Fig. 1. In Fig. 2, the number of background macroparticles is kept at a constant value of $N_p = 1024$. The dotted curve is from the self-consistent simulations, whereas the solid line is the analytical result given by $D = \alpha K^2$, where $\alpha = \bar{\xi}/N_p = 3.5 \times 10^{-4}$ ($\bar{\xi} = 0.35$). In Fig. 3, the coefficient D is plotted versus N_p, as obtained from self-consistent simulations of beam propagation through the same periodic focusing channel in Fig. 1 for a fixed value of $K = 0.5$. The dotted curve is from the self-consistent simulations, whereas the solid line is the analytical result given by $D = \beta K^2$, where $\beta = \bar{\xi} K^2 = 0.12$ ($\bar{\xi} = 0.48$). In comparison with Fig. 2, data fluctuations in Fig. 3 are larger because the initial distribution changes as N_p is varied. Nevertheless, it is evident in Fig. 2 and 3 that simulation results are in good agreement with the analytically predicted scaling law given in Eqs. (16) and (17).

To illustrate that the scaling law reported in this paper is a powerful result, we discuss two important applications of Eq. (18). As a first application, Eq. (18) is readily used to establish criteria for reliable self-consistent simulations. For example, let us specify an (allowed) error tolerance of 2% in the edge emittance in a simulation study of an intense beam propagating through 100 focusing periods with $SK/4\epsilon_{max}(0) = 10$. It follows from Eq. (18) that, in order to achieve the specified error tolerance, it is necessary to use at least $N_p \approx 3.5 \times 10^7$ particles in the simulation.

As a second application, Eq. (18) can be used to estimate beam losses due to discrete-particle effects. For example, let us consider an intense beam with $SK/4\epsilon_{max}(0) = 10$ propagating through a focusing channel with 100 periods and a transverse phase space acceptance of $1.5^2 \times (4\pi\epsilon)$, where $\epsilon = \epsilon_{max}(0)$. For $N_p = 3.5 \times 10^7$, we find from Eq. (18) that

$\epsilon_{max}(100S) = 1.02\epsilon_{max}(0)$. Assuming the edge particles [say, initially with $0.95 < A_{xi}(0) \leq 1$] obey a Gaussian distribution in the random variable $A_x - 1$ at $s = 100S$, the number of particles found outside the transverse phase space acceptance is of the order of $10^{-5}N_p$; that is, fractional particle loss due to discrete-particle effects is estimated to be 10^{-5}.

To summarize, we have obtained a scaling law for edge emittance growth induced by discrete-particle effects in two dimensional self-consistent simulations of intense charged-particle beams in a periodic solenoidal focusing field. The scaling law can be applied to establishing criteria for accurate self-consistent simulation studies of a variety of collective processes in periodically focused intense charged-particle beams, including beam halo formation and beam losses.

ACKNOWLEDGMENTS

One of the authors (C. C.) wishes to thank David Bruhwiler for stimulating discussions. This work was supported by Department of Energy, Grant No. DE-FG02-95ER-40919, and Air Force Office of Scientific Research, Grant Nos. F49620-94-1-0374 and F49620-97-1-0325. The research by R. Pakter was also supported by CAPES, Brazil.

REFERENCES

[1] M. Reiser, *Theory and Design of Charged-Particle Beams* (Wiley & Sons Inc., New York, 1994).

[2] *Space Charge Dominated Beams and Applications of High Brightness Beams*, edited by S Y. Lee, AIP Conf. Proc. **377** (AIP, New York, 1996).

[3] I. Hofmann, L. Laslett, L. Smith, and I. Haber, Part. Accel. **13**, 145 (1983).

[4] A. Friedman, D. P. Grote, and I. Haber, Phys. Fluids **B4**, 2203 (1992).

[5] J. Struckmeier and I. Hofmann, Part. Accel. **39**, 219 (1992).

[6] T. Chen, J. Irwin, and R. Siemann, Phys. Rev. **E49**, 2323 (1994).

[7] F. L. Krawczyk, J. H. Billen, R. D. Ryne, H. Takeda, and L. M. Young, in *Proceedings of the 1995 Particle Accelerator Conference* (IEEE, Piscataway, New Jersey, 1995), p. 2306, and references therein.

[8] C. Chen and R. A. Jameson, Phys. Rev. **E52**, 3074 (1995).

[9] R. W. Garnett, J. H. Billen, K. C. D. Chan, R. Genzlinger, E. R. Gray, S. Nath, R. Rusnak, D. L. Schrage, J. E. Stovall, H. Takeda, R. Wood, T. P. Wangler, and L. M. Young, AIP Conf. Proc. **377**, 60 (AIP, New York, 1996).

[10] H. Okamoto and M. Ikegami, Phys. Rev. **E55**, 4694 (1997).

[11] C. L. Bohn, Phys. Rev. Lett. **70**, 932 (1993).

[12] C. L. Bohn and J. R. Delayen, Phys. Rev. **E50**, 1516 (1994).

[13] J. Struckmeier, Phys. Rev. **E54**, 830 (1996).

[14] I. M. Kapchinskij and V. V. Vladimirskij, in *Proceedings of the International Conference on High Energy Accelerators* (CERN, Geneva, 1959), p. 274.

[15] C. Chen and R. C. Davidson, Phys. Rev. **E49**, 5679 (1994).

FIGURES

FIG. 1. Plot of $\sigma_A^2(s)/s^2$ versus the normalized propagation distance s obtained from the self-consistent simulation for $N_p = 1024$, $N_t = 512$, $K = 0.5$, and $\kappa_z(s) = [a_0 + a_1 \cos(2\pi s)]^2$, where $a_0 = a_1 = 0.648$. As indicated by the dashed line, the function $\sigma_A^2(s)/s^2$ reaches a plateau for $s > 1$, where the coefficient D is evaluated to be $D = 1.0 \times 10^{-4}$.

FIG. 2. Plot of the coefficient D versus K. Here, the value of N_p is fixed at $N_p = 1024$. The dotted curve is from self-consistent simulations, whereas the solid line is the analytical result given in Eq. (17) with a fitted value of $\alpha = \overline{\xi}/N_p = 3.5 \times 10^{-4}$ ($\overline{\xi} = 0.35$). Other parameters are the same as in Fig. 1.

FIG. 3. Plot of the coefficient D versus N_p. Here, the value of K is fixed at $K = 0.5$. The dotted curve is from self-consistent simulations, whereas the solid line is the analytical result given in Eq. (17) with a fitted value of $\beta = \overline{\xi}K^2 = 0.12$ ($\overline{\xi} = 0.48$). Other parameters are the same as in Fig. 1.

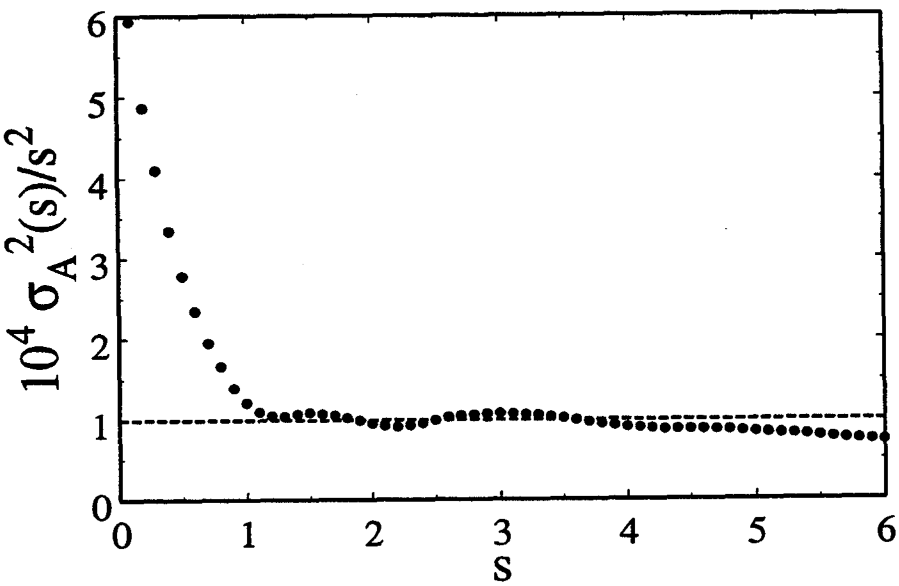

Figure 1
Pakter, Phys. Rev. Lett.

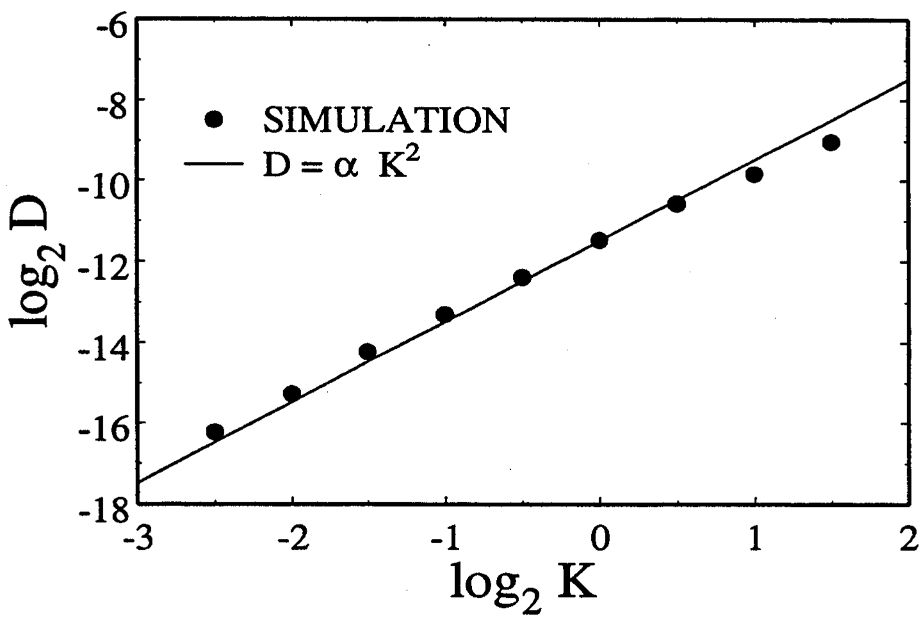

Figure 2
Pakter, Phys. Rev. Lett.

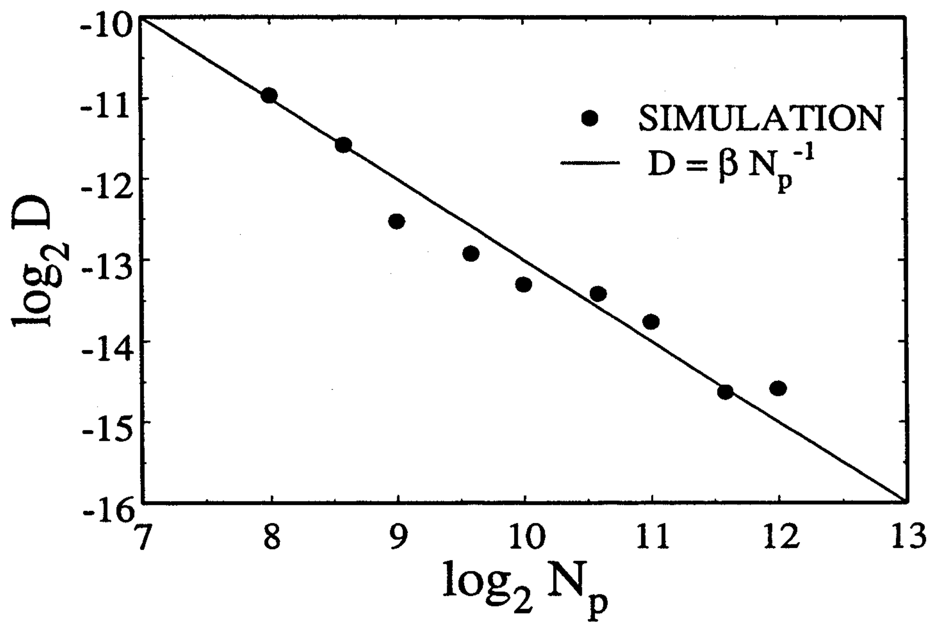

Figure 3
Pakter, Phys. Rev. Lett.